Research Square

Preprints are preliminary reports that have not undergone peer review.
They should not be considered conclusive, used to inform clinical practice,
or referenced by the media as validated information.

Health Risk Assessment of Airborne Endotoxin Associated with PM 10 in a Semi-Arid Region of the Indo-Gangetic Basin

Krishma Yadav
Dayalbagh Educational Institute (DEI)
Deeksha Rani
Dayalbagh Educational Institute (DEI)
Vaishnav Bartaria
Dayalbagh Educational Institute (DEI)
Ashok Yadav
Dayalbagh Educational Institute (DEI)
KK Mohanty
National JALMA Institute for Leprosy and other Mycobacterial Diseases (ICMR)
Ranjit Kumar
rkschem@rediffmail.com
Dayalbagh Educational Institute (DEI)

Research Article

Keywords: Airborne endotoxin, PM_{10}, Bioaerosol, Indo-Gangetic Basin, Seasonal variation, Health risk assessment, ADD, HQ, LAL assay

Posted Date: August 6th, 2026

DOI: https://doi.org/10.21203/rs.3.rs-10523351/v1

License: This work is licensed under a Creative Commons Attribution 4.0 International License. Read Full License

Additional Declarations: No competing interests reported.

Abstract

This study presents the first systematic assessment of ambient airborne endotoxin concentrations associated with coarse particulate matter (PM_{10}) in Agra, a semi-arid region over the Indo-Gangetic Basin (IGB), India, while simultaneously monitoring of bacterial and fungal bioaerosols, PM_{10}, and meteorological parameters throughout an entire calendar year (January-December 2022). The chromogenic endpoint Limulus Amebocyte Lysate (LAL) assay was used to quantify endotoxin. The monthly mean concentrations of endotoxin ranged from 0.92 ± 0.35 EU m^{-3} (June) to 7.35 ± 1.48 EU m^{-3} (December), exhibiting an ~ 8-fold seasonal amplitude driven by winter atmospheric stagnation. Spearman correlation analysis showed very significant positive correlation of endotoxin with bacterial concentration ($r_s = 0.93$, $p < 0.001$) and fungal concentration ($r_s = 0.98$, $p < 0.001$). A strong negative correlation between endotoxin and ambient temperature was observed ($r_s = -0.94$, $p < 0.001$). No significant correlation was found between PM_{10} and endotoxin ($r_s = 0.10$, $p = 0.746$), indicating that mineral dust is not the major carrier of endotoxin at this site. Health risk assessment for children, adult females, and adult males was made based on exposure-factor models of USEPA. Inhalation was the main exposure route with ADD values 3–4 times higher than dermal ADD. The hazard quotient (HQ) and hazard index (HI) values were well below unity for all groups during the year (max. HQ = 0.0198 for children in December), indicating acceptable non-carcinogenic risk compared to the Dutch Expert Committee on Occupational Standards (DECOS) reference dose of 90 EU m^{-3}. The findings emphasize the need to incorporate biological aerosol indicators into air-quality monitoring programs in the Indo-Gangetic Basin, since routine PM_{10} mass measurements may fail to fully account for seasonal fluctuations in airborne endotoxin exposure.

1. Introduction

Ambient air pollution is a major global health burden, and the biological components of airborne particulate matter are capturing increased scientific interest, along with their well-characterized chemical composition. Endotoxin (lipopolysaccharide, LPS), a structural element of the outer membrane of Gram-negative bacteria, becomes airborne when bacterial cells, cell fragments, or contaminated dust particles are resuspended into the atmosphere (Yoda et al., 2017; Liu et al., 2018). As a pervasive ubiquitous environmental contaminant present in organic aerosols, household dust, and ambient air, airborne endotoxin can affect large population groups (Liao et al. 2010).

Inhaled endotoxin is a potent pro-inflammatory agent for the respiratory tract. As a structural component of Gram-negative bacterial outer membranes, it is among the most potent bacterial inducers of cytokines including tumour necrosis factor (TNF), interleukin-1β (IL-1β), and gamma interferon (IFNγ) through activation of TLR4-mediated auto-amplificatory loops in monocytes and macrophages (Cavaillon et al., 2006).Chronic or excessive production of these cytokines triggers neutrophilic inflammation and bronchial hyper-responsivity even at relatively low ambient concentrations (Liebers et al., 2020; Thorne, 2021; Agarwal et al., 2023). Both occupational and general population studies have linked chronic endotoxin exposure to asthma exacerbations, allergic sensitisation, and respiratory morbidity (Farokhi et al. 2018; Shamsollahi et al. 2019a). Ambient endotoxin primarily associates with coarse particles (PM_{10}) and resuspended soil dust, though it can also adhere to $PM_{2.5}$ fractions (Heinrich et al., 2003; Behbod et al., 2013). In densely populated semi-arid

cities such as Agra, chronic exposure to high PM_{10} and $PM_{2.5}$ loads has been linked to cardiopulmonary mortality risk and substantial economic burden (Bartaria et al., 2026; Gupta et al., 2019; Kushwaha et al., 2025), highlighting the public health urgency of characterizing all biologically active components of ambient PM including endotoxin rather than relying solely on mass concentration metrics.

While endotoxin exposure has been characterized in diverse occupational settings including (Maharia & Srivastava, 2020) rice mills in northeast India where PM_{10} dust and endotoxin were strongly correlated (r^2 = 0.985, $p < 0.001$) (Kumar et al., 2024),rice mills in Indonesia(Dimjati Lusno et al. 2018) and university campuses (F. Liu 2025). A recent bibliometric analysis covering 1,469 publications from 72 countries (1971–2022) confirms that developing and low-income nations, particularly in South Asia, remain significantly underrepresented in ambient endotoxin research (Yadav et al., 2026). No study to date has characterized ambient endotoxin levels or associated health risks in India's Indo-Gangetic Basin (IGB). The IGB is among the world's most heavily polluted airsheds, characterized by dense population, high mineral dust loads, vehicular emissions, biomass burning, and intensive agriculture (Kumar et al., 2003; Bartaria et al., 2025a). Episodic emission events, such as festival-related pyrotechnics and biomass burning, further intensify particulate loads in the region (Bartaria et al., 2025a), and countrywide lockdown studies have confirmed that vehicular and industrial emissions are the primary drivers of IGB air quality variability (Gautam et al., 2021; Bartaria et al., 2025b). Elevated PM_{10} and $PM_{2.5}$ concentrations and their associated health and economic burdens have been extensively documented at Agra (Gupta et al., 2019; Kumar et al., 2020; Kushwaha et al., 2025), and year-round ground-based and satellite measurements confirm persistent black carbon and aerosol loading over this historic city (Bartaria et al. 2026). Seasonal characterization of $PM_{2.5}$ morphology and elemental composition in other Himalayan foothills and mountain valley sites further underlines the region-specific nature of aerosol sources in northern India (Nautiyal et al. 2025). Critically, bioaerosol studies conducted in Agra have documented abundant airborne bacterial and fungal communities in outdoor urban air throughout the year (Mamta et al. 2015; Raghav et al. 2020), with seasonal peaks in microbial aerosol concentrations driven by meteorological conditions analogous to those governing endotoxin variability in this study. These conditions persistent particulate pollution, active microbial communities, and seasonal atmospheric stagnation may intensify endotoxin-bearing particle concentrations, yet their temporal dynamics and associated health implications remain entirely unstudied in this region.

The present study addresses this gap at Agra, a representative IGB city. Its objectives are: (i) to quantify seasonal monthly PM_{10} associated airborne endotoxin and co-monitor bacteria, fungi, PM_{10}, and meteorological parameters; (ii) to analyse inter-parameter correlations and construct a full Spearman correlation heatmap; and (iii) to estimate inhalation and dermal ADD, HQ, and HI for children, adult females, and adult males using USEPA exposure-factor methodology.

2. Materials And Methods

2.1 Study Site and Sampling

Air sampling was conducted at the rooftop of a two-story building (~ 8 m above ground level) on the campus of Dayalbagh Educational Institute (DEI), Agra, shown in Fig. 1, a suburban site ~ 10 km from the industrial

zone and ~ 2 km from National Highway NH-19, having dense vehicular traffic. Samples were collected from January to December 2022, covering a full annual cycle and permitting seasonal variation analysis of PM_{10}. PM_{10} was collected using an Envirotech APM 460 BL sampler (flow rate: 1.0 m^3 min^{-1}; 24-h sampling duration (10 A.M. to 10 A.M. next day). Samples were collected weekly on Mondays throughout the year. Glass fiber filters (GFA) were used for PM_{10} because of their high filtration efficiency, to maintain chemical stability, and minimize hygroscopic interference. To keep consistent humidity levels, the filters were placed in a desiccator for 24 h, both prior to and following the sampling, and the weighing process was conducted under the same temperature and humidity conditions before and after the sampling. Subsequently, they were weighed using a microbalance (Contech analytical balance) to determine their initial and final weight (Bartaria et al., 2025). The PM concentration was determined using the following formula:

Concentration (μg m^{-3}) = Mass of filter paper (W_2 - W_1) / Total air volume (V) (m^3)

where W_1 is the initial weight of the filter before sampling (in grams), W_2 is the weight of the filter after sampling and the desiccator process (in grams), and V is the volume of air sampled (in, $m^{3)}$.

2.2 Endotoxin and Bioaerosol Analysis

Filters were preserved at 4°C for ≤ 2 h post-sampling to minimize LPS degradation and then analyzed to determine endotoxin levels (Duquenne et al., 2013). Endotoxin concentrations were quantified using the chromogenic Limulus Amebocyte Lysate (LAL) assay (96-well plate reader; detection limit: 0.1-1.0 EU/mL, QCL-1000, Biotek). Prior to analysis, all extracts and standards were brought to room temperature. For each sample, 50 µL of extract was mixed with an equal volume of LAL reagent in pyrogen-free microplate wells. The Reaction mixture was incubated at 37°C to activate the LAL protease cascade by endotoxin. Following the manufacturer's protocol, a chromogenic substrate was added and allowed to react before the enzymatic activity was quenched using 25% acetic acid. Absorbance measurements were performed at 405 nm using a microplate reader. Endotoxin concentrations (EU mL^{-1}) were derived from a standard calibration curve prepared with known LPS standards. EU mL^{-1} values were converted to total EU per filter based on extraction volumes and filter fractions, and then to EU m^{-3} using the measured air-sampling volume.

All glassware and consumables for LAL analysis were autoclaved to ensure absence of pyrogen contamination. Spike recovery and reagent blanks were run to ensure analytical accuracy.

Filter paper was biologically evaluated by culture techniques. A milliliter of the filtrate was used for fungal analysis on sterile SDA (Sabouraud dextrose agar) plates at 27°C for 3 days and for bacterial analysis the filtrate was used to inoculate NAM (nutrient agar medium) in a sterile petri plate and kept at 37°C for 3 days. The colony counts were made and after incubation period on SDA and NAM plates, sub cultures were made to get pure isolates of fungi and bacteria respectively. The shape, size and color of the colonies were observed under a light microscope and compared to standard descriptions to identify bacteria and fungi. Fungal and bacterial particles in the air are expressed as colony-forming units per cubic meter (CFU m-3). The field blank sample was collected and processed in the same manner as the aerosol samples. No microbial growth has been observed in the field blank sample.

2.3 Measurement of environmental parameters

Meteorological parameters, such as ambient temperature (°C), relative humidity (%), wind speed (ms^{-1}), and wind direction (°), were continuously recorded at one-minute intervals through an Automatic Weather Station (AWS) installed at a location approximately 5 m away from the aerosol sampling point. The meteorological characterization at this site has direct implications for the interpretation of PM_{10} concentration trends, transport mechanisms, dispersion patterns, and endotoxin variability. Agra's continental semi-arid climate features a pronounced seasonal cycle. Winter (December-February) is characterized by temperatures (4–12°C), weak westerly winds (~ 0.35–0.55 m/s), suppressed convective mixing, and a shallow planetary boundary layer (PBL) that results in accumulation of pollutants and bioaerosols near the surface (Gupta et al., 2023; Bartaria et al., 2026). These adverse meteorological conditions in the IGB during winter, including thermal inversions and reduced mixing height, are well-documented drivers of elevated particulate and biological aerosol concentrations (Bartaria et al., 2025b). In contrast, the pre-monsoon season (March-May) is characterized by high temperatures (28–40°C) and strong convective mixing that dilutes bioaerosol concentrations, while monsoon months (June-September) bring elevated relative humidity (60–78%) and wet-scavenging of particles.

2.3 Health Risk Assessment Framework

The modes of exposure to airborne endotoxins include skin contact(Li et al. 2013) and inhalation (Rennie et al. 2008).Average Daily Dose (ADD) rates via inhalation and dermal contact were estimated using the United States Environmental Protection Agency (USEPA) Exposure Factors Handbook(Epa and Factors Program, 2011) models validated in prior bioaerosol studies(Li et al. 2013; H. Liu et al. 2018) using Equation given below. Average Daily Dose (ADD) rates via inhalation and dermal contact were estimated using the USEPA Exposure Factors Handbook(Epa and Factors Program, 2011) models validated in prior bioaerosol studies (Li et al. 2013; H. Liu et al. 2018)

$$ADD_{inhalation} = c \times IR \times EF \times ET / (BW \times AT)$$

$$ADD_{skin} = c \times S_A \times P_c \times EF \times ET \times 24 / (BW \times AT)$$

where c = ambient endotoxin concentration (EU m^{-3}); IR = inhalation rate (7.6/14.17/19.02 m^3/d for children/adult females/adult males); EF = exposure frequency (350 d/a); ET = exposure time (6 a children, 24 a adults); BW = body weight (15.0/54.4/62.7 kg); AT = averaging time (12 × 365, 73.3 × 365, 69.6 × 365 d); S_A = 0.115/0.215 m^2; P_c = 0.001 m/h (Epa and Factors Program, 2011).The dose rates were assessed using the average concentrations of airborne endotoxin.

Aerosolized endotoxins are not carcinogenic(H. Liu et al. 2018). Consequently, the hazard index (HI) was employed to evaluate health risk. ADD was subsequently contrasted with the reference dose (RfD). The potential danger posed by noncarcinogens to the exposed demographic was subsequently evaluated and represented quantitatively as a probabilistic risk profile (USEPA, 2011) as detailed below:

$$HQ = ADD / RfD \quad ....3$$

$$HI = \Sigma HQ_i \quad ....4$$

A reference dose (RfD) of 90 EU m^{-3} was established in accordance with the guidance of the Dutch Expert Committee on Occupational Standards (DECOS, 2010). This reference dose was used because no defined ambient reference value for endotoxin exposure in the general population exists. A validated general-population reference standard for endotoxin exposure has been created. Comparable methodologies have been employed to evaluate ambient and community bioaerosol hazards (Hwang and Park 2019; H. Liu et al. 2018). HQ/HI < 1 indicates acceptable risk; HQ/HI > 1 indicates potential hazard. Spearman's rank correlations were computed in IBM SPSS 22 (significance threshold: $p < 0.05$) following established practices in bioaerosol risk research(Liu et al., 2018; Shamsollahi et al., 2019).

3. Results And Discussion

3.1 Monthly Airborne Endotoxin Concentrations

Monthly descriptive statistics for airborne endotoxin concentrations at Agra are presented in Table 1 and Fig. 2. There is a clear seasonal cycle with peaks in concentration in December (7.35 ± 1.48 EU m^{-3}) and November (6.98 ± 1.25 EU m^{-3}) and a winter cluster (December–February mean: 6.55 EU m^{-3}) that is about 7–8 times higher than the summer minimum (June: 0.92 ± 0.35 EU m^{-3}). The highest individual concentration was 9.85 EU m^{-3} (December) and the lowest 0.48 EU m^{-3} (June). The annual mean was 3.77 ± 2.22 EU m^{-3}, which is much lower than the DECOS reference dose of 90 EU m^{-3}. The large winter accumulation is in line with the wintertime atmospheric dynamics in the IGB, namely low boundary layer heights, thermal inversions, reduced convective mixing, and suppressed photochemical LPS degradation, which all contribute to longer residence times of particles and concentration of bioaerosol-laden particles near the surface (Yoda et al., 2017; Maharia and Srivastava, 2020). A transitional decrease was seen from March (3.95 EU m^{-3}) to April (2.11 EU m^{-3}) to the summer minimum (May-June). During monsoon season (July-September), a small rebound (1.48–2.87 EU m^{-3}) was observed due to variability in atmospheric moisture and surface conditions. Post-monsoon months (October-November) showed a progressive rise as temperatures cooled and atmospheric stability increased. The seasonal box-plot (Fig. 2) illustrates that standard deviation values were highest in winter (1.12–1.48), indicating greater inter-event variability likely driven by variable biomass-burning intensity and cold-wave episodes, and lowest in summer (0.35–0.54), reflecting stable conditions. Comparison with worldwide studies (Table 2) reveals that the annual mean endotoxin concentration at Agra (3.77 EU m^{-3}) is among the highest ambient values reported globally, reflecting the exceptionally high bioaerosol burden and atmospheric stagnation characteristic of the IGB. In contrast, most temperate-zone urban ambient studies have reported winter minima and summer/spring maxima, the opposite of what was observed here, because bacterial growth on organic substrates is thermally stimulated at higher temperatures in those climates (Carty et al., 2003; Heinrich et al., 2003). Studies from Munich, Germany, reported endotoxin levels in $PM_{2.5}$ peaking in spring and summer (geometric mean: 0.015 EU m^{-3}), with a strong positive correlation with ambient temperature ($r = 0.641$, $p < 0.0001$) (Carty et al., 2003). Similarly, ambient endotoxin studies in British Columbia, Canada, found concentrations generally highest in summer and fall, lowest in winter and spring, with temperature and relative humidity identified as the most influential meteorological parameters (Allen et al., 2011). South Korean ambient data showed a geometric mean of 0.132 EU m^{-3} with endotoxin levels significantly higher in autumn and winter than in summer (Hwang and Park, 2019), consistent

with the seasonal reversal seen in the present study. In Beijing, China, geometric mean endotoxin in $PM_{2.5}$ ranged from 8.35 to 11.31 EU m^{-3} across seasons with spring peaks (Guan et al., 2014 cited in Chong et al., 2024), substantially higher than concentrations at Agra, likely due to intense agricultural activities and dust storms. A study from Chitwan, Nepal the nearest South Asian ambient comparison reported PM_{10}-associated endotoxin concentrations of 0.29–0.53 EU m^{-3} during summer 2016, with meteorological variables having limited influence apart from relative humidity (Gorris et al., 2017). The consistently higher values at Agra relative to most non-occupational settings underscore the need for region-specific endotoxin monitoring in high-PM South Asian environments. Crucially, the inverse seasonal pattern (winter peak instead of summer peak) observed at Agra is a defining feature driven by IGB-specific meteorology low boundary layer, thermal inversions, and biomass burning stagnation rather than temperature-driven bacterial growth.

Table 1
Monthly descriptive statistics of airborne endotoxin concentrations (EU m^{-3}) with seasonal classification, plus corresponding bacterial and fungal bioaerosol concentrations (CFU m^{-3}) and bacteria-to-fungi ratio.

Month	Season	Mean (EU m^{-3})	SD	Min-Max (EU m^{-3})	Bacteria (CFU m^{-3})	Fungi (CFU m^{-3})	Bacteria: Fungi Ratio
January	Winter	6.42	1.12	5.01–8.02	910 ± 85	360 ± 40	2.53
February	Winter	5.88	0.96	4.7–7.21	720 ± 70	300 ± 35	2.40
March	Pre-summer	3.95	0.82	2.9–5.1	540 ± 60	240 ± 30	2.25
April	Summer	2.11	0.54	1.4–3.01	410 ± 55	190 ± 28	2.16
May	Summer	1.34	0.41	0.82–2.1	320 ± 50	140 ± 25	2.29
June	Summer	0.92	0.35	0.48–1.56	260 ± 45	110 ± 20	2.36
July	Monsoon	1.48	0.52	0.9–2.3	210 ± 40	125 ± 22	1.68
August	Monsoon	1.76	0.63	0.95–2.95	240 ± 42	130 ± 24	1.85
September	Post-monsoon	2.87	0.71	1.9–4.02	380 ± 55	210 ± 30	1.81
October	Post-monsoon	4.21	0.88	3.02–5.8	650 ± 75	290 ± 35	2.24
November	Early Winter	6.98	1.25	5.22–9.01	880 ± 90	370 ± 42	2.38
December	Winter	7.35	1.48	5.6–9.85	940 ± 95	380 ± 45	2.47

Table 2
Comparison of ambient/near-ambient airborne endotoxin concentrations from the present study with published studies worldwide.

Study Location	Environment / PM Fraction	Endotoxin Conc. (EU m^{-3})	Seasonal Peak	Method	Reference
Agra, India (Present Study)	Outdoor ambient / PM_{10}	0.92–7.35 (mean 3.77)	Winter (Dec)	LAL chromogenic; Envirotech APM 460	This study
Chinese university campus (China)	Outdoor ambient / PM_{10}	0.22–3.78	Summer/Autumn	LAL kinetic	Liu et al. (2018)
Delhi STP, India	Sewage treatment plant / PM_{10} - $PM_{2.5}$	2.0-9.5	Summer (high temp.)	LAL; cascade impactor	Maharia & Srivastava (2020)
South Korea (ambient)	Outdoor ambient / PM_{10}, $PM_{2.5}$	0.1–1.5 (GM: 0.132)	Fall/Winter	LAL kinetic	Hwang & Park (2019)
Munich, Germany	Outdoor ambient / $PM_{2.5}$	GM: 0.015	Spring/Summer	LAL kinetic chromogenic	Carty et al. (2003)
Chitwan, Nepal	Outdoor ambient / PM_{10}	0.29–0.53	RH-dependent (summer)	LAL; E-sampler	Mahapatra et al. (2017)
NE India (rice mill workers)	Occupational (indoor) / PM_{10}	GM: 2.2 (up to 17.8)	Year-round (occupational)	LAL chromogenic; Envirotech APM 460	Kumar Chhetry et al. (2024)

Note: GM = geometric mean; STP = sewage treatment plant; LAL = Limulus Amebocyte Lysate; RH = relative humidity.

3.2 Monthly Bacterial and Fungal Bioaerosol Concentrations

The monthly concentration of bacterial and fungal bioaerosols is summarized in Table 1 and shown in Fig. 2B. Both the bioaerosol components showed a seasonal profile very similar to that of endotoxin, with maximum concentrations in winter and minima during the monsoon season. The total airborne bacteria varied from 210 ± 40 CFU m^{-3} (July) to 940 ± 95 CFU m^{-3} (December) and fungi from 110 ± 20 CFU m^{-3} (June) to 380 ± 45 CFU m^{-3} (December). The ratio of bacteria to fungi was relatively constant across months (~ 2.4–2.5:1), indicating co-transport on a common aerosol matrix.

Reduced atmospheric mixing, slower microbial die-off at lower temperatures, and persistent biomass burning, which resuspends soil-associated organisms, have been attributed to winter accumulation of bacteria and fungi in the IGB (Maharia and Srivastava, 2020). The almost simultaneous seasonal peaks of bacteria, fungi and endotoxin support the interpretation that endotoxin is largely derived from and transported together with

Gram-negative bacterial cells resuspended from soil surfaces and organic waste, a key finding statistically confirmed by the correlation analysis in Section 3.4

3.3 PM_{10}, and Meteorological Parameter Profiles

Monthly concentrations of PM_{10} are shown in Fig. 2A. The seasonal pattern of PM_{10} was bimodal, typical of IGB, with maximum values in April (254.8 μg m^{-3}) due to pre-monsoon dust storms and minimum values in August (46.7 μg m^{-3}) due to monsoon wet-scavenging. The meteorological conditions are shown in the 4-panel plot (Fig. 3). Ambient temperature ranged from 13.2°C (January) to 34.0°C (June) with relative humidity from 23.1% (April, peak dry season) to 78.0% (August, peak monsoon) and wind speed from 0.35 m/s (February) to 1.68 m/s (June).

Interestingly, PM_{10} and endotoxin exhibited very different seasonal cycles. PM_{10} peaked in spring (April) but endotoxin peaked in winter (December) indicating that mineral dust resuspension and accumulation of biological endotoxin are driven by fundamentally different environmental drivers as explained in section 3.4.

3.4 Spearman Correlation Analysis and Heatmap

The Spearman's rank correlation coefficients between airborne endotoxin and all measured parameters are shown in the full correlation heatmap in Fig. 4. Figure 5 shows pairwise scatter plots for key relationships. Endotoxin correlated positively and most strongly with fungal concentration ($r_s = 0.979$, $p < 0.001$) and bacterial concentration ($r_s = 0.930$, $p < 0.001$). These near-perfect associations validate bacterial and fungal bioaerosols as the primary sources and co-transport vehicles of endotoxin at this site. The bacterial and fungal communities were also highly correlated ($r_s = 0.965$, $p < 0.001$), in agreement with their common soil and organic substrate origins.

The strongest negative correlation was found for ambient temperature ($r_s = -0.944$, $p < 0.001$), which confirms the dominant role of cold-season atmospheric stability in the promotion of endotoxin accumulation. Similarly high negative correlations of bacteria and fungi with temperature were observed ($r_s = -0.902$ and -0.951, respectively), reinforcing the fact that all three biological contaminants accumulate simultaneously during winter thermal inversions.

PM_{10} was not significantly correlated with endotoxin ($r_s = 0.105$, $p = 0.746$). This unexpected finding, in contrast with some European and Chinese studies (Heinrich et al., 2003; Liu et al., 2018), and in stark contrast to Indian rice mill occupational environments, where PM_{10} dust and endotoxin are near-perfectly correlated ($r^2 = 0.985$, $p < 0.001$) (Kumar Chhetry et al., 2024), reflects the decoupling of mineral dust and biological endotoxin seasonal cycles in this semi-arid IGB environment. The maximum levels of PM_{10} are found during the hot and dry pre-monsoon season (April) when mineral dust is suspended in the air. The maximum levels of endotoxin are found in winter, due to biological accumulation and atmospheric stagnation. This discrepancy has important implications: PM_{10}-based proxies are not sufficient to characterize biological endotoxin burden in this setting. Endotoxin was not significantly correlated with relative humidity and wind speed ($p > 0.05$).

3.5 Average Daily Dose (ADD) via Inhalation and Skin Contact

The estimated monthly ADD values of inhalation and dermal for the three population groups are presented in Tables 3 and shown in Fig. 6. On a log scale (Fig. 7), the comparison of both pathways clearly shows that inhalation ADD was 3–4 orders of magnitude higher than skin contact ADD in all groups and all months.

Table 3
Monthly Average Daily Dose (ADD, EU d^{-1} kg^{-1}) via inhalation and skin contact for three population groups (children, adult females, and adult males).

Month	$ADD_{inhalation}$ (EU/d/kg)			ADD_{skin} (EU/d/kg)		
	Children	Adult Females	Adult Males	Children	Adult Females	Adult Males
January	1.559562	0.525035	0.643954	5.664e-4	1.912e-4	1.747e-4
February	1.428384	0.480873	0.589790	5.187e-4	1.751e-4	1.600e-4
March	0.959543	0.323036	0.396203	3.485e-4	1.176e-4	1.075e-4
April	0.512566	0.172558	0.211642	1.861e-4	6.284e-5	5.742e-5
May	0.325516	0.109587	0.134408	1.182e-4	3.991e-5	3.646e-5
June	0.223489	0.075239	0.092280	8.116e-5	2.740e-5	2.503e-5
July	0.359525	0.121036	0.148451	1.306e-4	4.408e-5	4.027e-5
August	0.427543	0.143935	0.176536	1.553e-4	5.241e-5	4.789e-5
September	0.697187	0.234712	0.287874	2.532e-4	8.547e-5	7.810e-5
October	1.022703	0.344299	0.422282	3.714e-4	1.254e-4	1.146e-4
November	1.695598	0.570833	0.700125	6.158e-4	2.079e-4	1.899e-4
December	1.785479	0.601092	0.737238	6.484e-4	2.189e-4	2.000e-4

Children of all the population groups consistently showed the highest inhalation ADD with the highest value of 1.7855 EU/d/kg recorded in December. This was due to the significantly higher inhalation rate per unit body weight (IR/BW = 7.6/15.0 = 0.507 m^3/d/kg) than adult males (19.02/62.7 = 0.303 m^3/d/kg) and adult females (14.17/54.4 = 0.260 m^3/d/kg). Despite heavier BW, adult males had the second highest inhalation ADD due to higher IR. Seasonal profiles of ADD were in good agreement with trends in endotoxin concentration with maxima in winter (December-January) and minima in summer (June).

The dermal ADD values ranged from 8.1×10^{-5} EU/d/kg (children, June) to 6.5×10^{-4} EU/d/kg (children, December), which is over 2,700 times lower than the respective inhalation ADD. This small dermal contribution is indicative of the very low skin permeability coefficient for LPS (Pc = 0.001 m/h) and the limited exposed skin surface areas assumed in the model (Epa and Factors Program, 2011). These results confirm the predominance of inhalation as an exposure pathway, in agreement with the bioaerosol risk assessment in other environments (Liu et al., 2018).

3.6 Hazard Quotient (HQ), Hazard Index (HI), and Risk Interpretation

Monthly HQ and HI values are presented in Table 4. All HQ and HI values for both exposure pathways and all population groups remained well below unity throughout the entire monitoring period, indicating acceptable non-carcinogenic risk levels relative to the DECOS RfD of 90 EU m^{-3}.

Table 4
Monthly Hazard Quotient (HQ) via inhalation and skin contact, with corresponding Hazard Index (HI), for three population groups (RfD = 90 EU m^{-3}).

Month	$HQ_{inhalation}$ & HI				HQ_{skin} & HI			
	Children	Adult Females	Adult Males	$HQ_{inhalation}$	Children	Adult Females	Adult Males	HI_{skin}
January	0.01733	0.00583	0.00716	0.03032	6.293e-6	2.124e-6	1.941e-6	1.036e-5
February	0.01587	0.00534	0.00655	0.02777	5.764e-6	1.946e-6	1.778e-6	9.487e-6
March	0.01066	0.00359	0.00440	0.01865	3.872e-6	1.307e-6	1.194e-6	6.373e-6
April	0.00570	0.00192	0.00235	0.00996	2.068e-6	6.982e-7	6.380e-7	3.404e-6
May	0.00362	0.00122	0.00149	0.00633	1.313e-6	4.434e-7	4.052e-7	2.162e-6
June	0.00248	0.00084	0.00103	0.00434	9.018e-7	3.044e-7	2.782e-7	1.484e-6
July	0.00399	0.00134	0.00165	0.00699	1.451e-6	4.897e-7	4.475e-7	2.388e-6
August	0.00475	0.00160	0.00196	0.00831	1.725e-6	5.824e-7	5.321e-7	2.840e-6
September	0.00775	0.00261	0.00320	0.01355	2.813e-6	9.497e-7	8.678e-7	4.631e-6
October	0.01136	0.00383	0.00469	0.01988	4.127e-6	1.393e-6	1.273e-6	6.793e-6
November	0.01884	0.00634	0.00778	0.03296	6.842e-6	2.310e-6	2.110e-6	1.126e-5
December	0.01984	0.00668	0.00819	0.03471	7.205e-6	2.432e-6	2.222e-6	1.186e-5

The maximum inhalation HQ was recorded for children in December ($HQ_{inhalation}$ = 0.01984), followed by November (HQinhalation = 0.01884). Even at peak winter concentrations, inhalation HQ values were more than 50-fold below the risk threshold of unity. Adult males and females consistently showed lower HQ values than children across all months due to their lower inhalation rate per unit body weight. The highest HQ_{skin} was also recorded for children in December (3.61×10^{-6}), which is more than 5 orders of magnitude below the risk threshold.

The combined HI (inhalation + skin contact) was entirely dominated by the inhalation component, with skin contact contributing < 0.02% of total HI for all groups and months. $HQ_{inhalation}$ ranged from 0.00434 (June) to 0.03471 (December), while HI_{skin} ranged from 1.48×10^{-6} to 1.19×10^{-5}. These findings demonstrate that even cumulative multi-pathway exposures pose no meaningful risk at present ambient endotoxin levels. These values are broadly comparable to HQ values reported from Chinese university campuses (H. Liu et al. 2018)and Korean ambient environments (Hwang and Park 2019) where HQ values similarly remained below unity in non-occupational settings.

Since HQ = ADD/RfD and ADD is directly proportional to ambient endotoxin concentration, HQ and HI are perfectly linearly correlated with monthly endotoxin values ($r_s = 1.000$, $p < 0.001$ for all groups), meaning the seasonal pattern of endotoxin exposure entirely governs the temporal dynamics of non-carcinogenic health risk at this site. Despite current HQ < 1 values, the pronounced winter-season endotoxin burden (December values ~ 8-fold above June) underscores the need for targeted public health advisories during cold months, particularly for susceptible sub-populations including children, the elderly, and individuals with pre-existing respiratory conditions (asthma, COPD) who may exhibit heightened inflammatory responses at lower endotoxin thresholds(Farokhi et al. 2018; Thorne 2021).

3.7 Environmental and Public Health Implications

The findings of this study have important implications for air-quality management and public health in the Indo-Gangetic Basin. The high levels of endotoxin in the air during winter in Agra, although still below the threshold level considered safe for workers, indicate that biological material in the dust and soot may contribute to respiratory problems in people who are constantly breathing it. The strong association of endotoxin with airborne bacterial and fungal aerosols, and the lack of a strong association with PM_{10} mass, suggest that monitoring of traditional particulate mass alone may not adequately reflect exposure to biologically active aerosols. The findings underscore the need to incorporate bioaerosol and endotoxin measurements in routine air-quality surveillance programs across the Indo-Gangetic Basin. Such monitoring may help address respiratory-health risks, provide early warning systems during winter pollution episodes, and inform the development of more comprehensive air-quality management strategies in rapidly urbanizing regions of South Asia.

4. Conclusion

A first systematic assessment of ambient airborne endotoxin and related health risks in the Indo-Gangetic Basin at Agra shows a strong seasonal variation, with concentrations increasing about eight times from a summer minimum of 0.92 ± 0.35 EU m^{-3} in June to a winter maximum of 7.35 ± 1.48 EU m^{-3} in December. The main reasons for this pattern are atmospheric stagnation in the cold season and increased biological accumulation under stable boundary layer conditions. Endotoxin concentrations were very strongly positively correlated with bacterial ($r_s = 0.930$, $p < 0.001$) and fungal ($r_s = 0.979$, $p < 0.001$) bioaerosol levels; this close association indicates that endotoxins are likely to be co-transported with microbial components. PM_{10} was not significantly correlated with endotoxin ($r = 0.105$, $p = 0.746$), indicating that bulk particulate mass is not a good surrogate for endotoxin variability in this semi-arid setting. Among the meteorological variables, ambient temperature was the most dominant driver with a strong negative correlation ($r = -0.944$, $p < 0.001$),

consistent with the role of wintertime atmospheric stability in the accumulation of pollutants. The health risk assessment also confirmed that inhalation is the major route of exposure, with the ADDinhalation values being 3–4 orders of magnitude higher than the dermal exposure for all population groups. Children had the highest exposure and risk levels among the population groups due to their higher inhalation rate per unit body weight. However, even with seasonal variation, all calculated HQ and HI values were far below unity throughout the study period, with a maximum of 0.0198 for children in December, signifying an acceptable non-carcinogenic health risk under current ambient conditions based on the DECOS reference dose of 90 EU m^{-3}.

We present the first ambient endotoxin baseline for the Indo-Gangetic Basin and show that biological aerosol dynamics are strongly influenced by regional meteorology and microbial abundance, not just by particulate mass concentration. These results imply that typical air quality assessments based solely on PM metrics may underestimate the biologically mediated respiratory exposure in winter pollution events.Future monitoring programs should include measurements of endotoxin and bioaerosols in addition to traditional particulate pollutants to provide a fuller assessment of population exposure and to help inform evidence-based public-health interventions in heavily polluted South Asian urban environments.

Declarations

CRediT authorship contribution statement: Krishma Yadav: Conceptualization, Methodology, Investigation, Data curation, Formal analysis, Writing - original draft.
Vaishnav Bartaria: Conceptualization, Data interpretation, Validation, Writing - review & editing. Deeksha: Investigation, Laboratory analysis, Data curation.
Ashok Yadav: Methodology, Instrumentation support, Supervision. KK Mohanty: Instrumentation support. Ranjit Kumar: Conceptualization, Supervision, Project administration, Writing - review & editing.

Declaration of competing interest: The authors declare that they have no known competing financial interests or personal relationships that could have appeared to influence the work reported in this paper.

Funding: This research receives partial financial support from ISRO GBP ARFI Project.
Data availability: The data that support the findings of this study are available from the corresponding author upon reasonable request.

Acknowledgements: The authors gratefully acknowledge the support provided by the Department of Chemistry and the Department of Civil Engineering, Dayalbagh Educational Institute (DEI), Agra, for laboratory facilities and sampling support. Financial support from ISRO-GBP ARFI Project highly acknowledged.

Ethical approval: This study does not involve human participants, animal experiments, or any ethical concerns requiring approval.

Consent for publication: All authors have read and approved the final manuscript and agree to its submission for publication.

References

1. Agarwal, V., Yue, Y., Zhang, X., Feng, X., Tao, Y., & Wang, J. (2023). Spatial and temporal distribution of endotoxins, antibiotic resistance genes and mobile genetic elements in the air of a dairy farm in Germany. Environmental Pollution, 336. https://doi.org/10.1016/j.envpol.2023.122404
2. Bartaria, V., Jangid, A., & Kumar, R. (2025a). Air quality dynamics and health risks: particle morphology and chemistry during pre and post-holi festival in a Tourist City in India. Air Quality, Atmosphere and Health, 18(7), 2031–2046. https://doi.org/10.1007/s11869-025-01751-2
3. Bartaria, V., Jangid, A., & Kumar, R. (2025b). Pyrotechnic impact of Diwali 2023 on black carbon and aerosol levels in Taj City, India: Relative endangerments and meteorological influences. Urban Climate, 61. https://doi.org/10.1016/j.uclim.2025.102386
4. Bartaria, V., Jangid, A., & Kumar, R. (2025c). Pyrotechnic impact of Diwali 2023 on black carbon and aerosol levels in Taj City, India: Relative endangerments and meteorological influences. Urban Climate, 61. https://doi.org/10.1016/j.uclim.2025.102386
5. Bartaria, V., Jangid, A., & Kumar, R. (2026). Year (2024–25)-bound assessment of PM and Black Carbon variability over historic city in India: insights from ground-based measurements and satellite data. International Journal of Remote Sensing. https://doi.org/10.1080/01431161.2025.2602840
6. Behbod, B., Urch, B., Speck, M., Scott, J. A., Liu, L., Poon, R., et al. (2013). Endotoxin in concentrated coarse and fine ambient particles induces acute systemic inflammation in controlled human exposures. Occupational and Environmental Medicine, 70(11), 761–767. https://doi.org/10.1136/oemed-2013-101498
7. Cavaillon, J.-M., Popoff, M. R., Khoury, J., Dabbousy, R., Hraoui-Bloquet, S., Sadek, R., et al. (n.d.). THE AQUEOUS BUDS EXTRACT OF EUCALYPTUS NEUTRALIZES THE MAIN ENZYMATIC ACTIVITIES OF MONTIVIPERA BORNMUELLERI VENOM.
8. Dimjati Lusno, M. F., Candraning Diyanah, K., & Keman, S. (2018). Lipopolysaccharides Endotoxin-containing Paddy Dust Leads to Cross-shift Lung Function Decline and Respiratory Complaints in Paddy Milling Machine Operators. KnE Life Sciences, 4(4), 442. https://doi.org/10.18502/kls.v4i4.2305
9. Duquenne, P., Marchand, G., & Duchaine, C. (2013, March). Measurement of endotoxins in bioaerosols at workplace: A critical revie. Annals of Occupational Hygiene. https://doi.org/10.1093/annhyg/mes051
10. Epa, U., & Factors Program, E. (n.d.). Exposure Factors Handbook: 2011 Edition. www.epa.gov
11. Farokhi, A., Heederik, D., & Smit, L. A. M. (2018, February 8). Respiratory health effects of exposure to low levels of airborne endotoxin - A systematic review. Environmental Health: A Global Access Science Source. BioMed Central Ltd. https://doi.org/10.1186/s12940-018-0360-7
12. Gautam, A. S., Kumar, S., Gautam, S., Anand, A., Kumar, R., Joshi, A., et al. (2021). Pandemic induced lockdown as a boon to the Environment: trends in air pollution concentration across India. Asia-Pacific Journal of Atmospheric Sciences, 57(4), 741–756. https://doi.org/10.1007/s13143-021-00232-7
13. Gupta, P., Jangid, A., & Kumar, R. (2019). Measurement of PM10, PM2.5 and black carbon and assessment of their health effects in Agra, A Semiarid Region of India. Proceedings of the Indian National Science Academy, 85(3), 667–679. https://doi.org/10.16943/ptinsa/2019/49677
14. Heinrich, J., Pitz, M., Bischof, W., Krug, N., & Borm, P. J. A. (2003). Endotoxin in fine (PM2.5) and coarse (PM2.5-10) particle mass of ambient aerosols. A temporo-spatial analysis. Atmospheric Environment, 37(26), 3659–3667. https://doi.org/10.1016/S1352-2310(03)00467-9

15. Hwang, S. H., & Park, D. U. (2019). Ambient endotoxin and chemical pollutant (Pm10, pm2.5, and o3) levels in south korea. Aerosol and Air Quality Research, 19(4), 786–793. https://doi.org/10.4209/aaqr.2018.06.0235
16. Kumar Chhetry, B. S., Tada, T., Dewangan, K. N., & Kumar, P. (2024). Evaluation of dust and endotoxin exposure among rice mill workers in northeast India. Toxicon, 248. https://doi.org/10.1016/j.toxicon.2024.108050
17. Kumar, R., Gupta, P., & Jangid, A. (2020). An empirical study towards air pollution control in Agra, India: a case study. SN Applied Sciences, 2(12). https://doi.org/10.1007/s42452-020-03826-4
18. Kumar, R., Rani, A., Kumari, K. M., & Srivastava, S. S. (2003). Direct measurement of atmospheric dry deposition to natural surfaces in a semiarid region of north central India. Journal of Geophysical Research Atmospheres, 108(20). https://doi.org/10.1029/2002JD003194
19. Kushwaha, D., Saxena, S. P., & Kumar, R. (2025a). Estimating health and economic burden of PM10 pollution in Agra, India using AirQ + and VSL approaches. Scientific Reports, 15(1). https://doi.org/10.1038/s41598-025-09137-1
20. Kushwaha, D., Saxena, S. P., & Kumar, R. (2025b). Estimating health and economic burden of PM10 pollution in Agra, India using AirQ + and VSL approaches. Scientific Reports, 15(1). https://doi.org/10.1038/s41598-025-09137-1
21. Li, Y., Zhang, H., Qiu, X., Zhang, Y., & Wang, H. (2013). Dispersion and risk assessment of bacterial aerosols emitted from rotating-brush aerator during summer in a wastewater treatment plant of xi'an, china. Aerosol and Air Quality Research, 13(6), 1807–1814. https://doi.org/10.4209/aaqr.2012.09.0245
22. Liao, V. H. C., Chio, C. P., Chou, W. C., Ju, Y. R., & Liao, C. M. (2010). Modeling human health risks of airborne endotoxin in homes during the winter and summer seasons. Science of the Total Environment, 408(7), 1530–1537. https://doi.org/10.1016/j.scitotenv.2010.01.007
23. Liebers, V., Brüning, T., & Raulf, M. (2020, November 1). Occupational endotoxin exposure and health effects. Archives of Toxicology. Springer Science and Business Media Deutschland GmbH. https://doi.org/10.1007/s00204-020-02905-0
24. Liu, F. (2025, October 1). Safety assessment of endotoxin related to drug products and medical devices: A review. Toxicology Letters. Elsevier Ireland Ltd. https://doi.org/10.1016/j.toxlet.2025.08.012
25. Liu, H., Zhang, Z., Wen, N., & Wang, C. (2018). Determination and risk assessment of airborne endotoxin concentrations in a university campus. Journal of Aerosol Science, 115, 146–157. https://doi.org/10.1016/j.jaerosci.2017.09.002
26. Maharia, S., & Srivastava, A. (2020). Seasonal effects in endotoxin concentration at different sections of a sewage treatment plant, Delhi. Aerobiologia, 36(3), 449–458. https://doi.org/10.1007/s10453-020-09644-w
27. Mamta, Shrivastava, J. N., Satsangi, G. P., & Kumar, R. (2015). Assessment of bioaerosol pollution over Indo-Gangetic plain. Environmental Science and Pollution Research, 22(8), 6004–6009. https://doi.org/10.1007/s11356-014-3776-9
28. Nautiyal, S. N., Joshi, V., Gautam, A. S., Kumar, R., Kumar, S., Singh, K., & Gautam, S. (2025). Characterization and source apportionment of PM2.5 and PM10 in a Mountain Valley: seasonal

variations, morphology, and elemental composition. Journal of Atmospheric Chemistry, 82(1). https://doi.org/10.1007/s10874-025-09469-2

29. Raghav, N., Mamta, Shrivastava, J. N., Satsangi, G. P., & Kumar, R. (2020). Enumeration and characterization of airborne microbial communities in an outdoor environment of the city of Taj, India. Urban Climate, 32. https://doi.org/10.1016/j.uclim.2020.100596
30. Rennie, D. C., Lawson, J. A., Kirychuk, S. P., Paterson, C., Willson, P. J., Senthilselvan, A., & Cockcroft, D. W. (2008). Assessment of endotoxin levels in the home and current asthma and wheeze in school-age children. Indoor Air, 18(6), 447–453. https://doi.org/10.1111/j.1600-0668.2008.00543.x
31. Shamsollahi, H. R., Ghoochani, M., Jaafari, J., Moosavi, A., Sillanpää, M., & Alimohammadi, M. (2019a, June 15). Environmental exposure to endotoxin and its health outcomes: A systematic review. Ecotoxicology and Environmental Safety. Academic Press. https://doi.org/10.1016/j.ecoenv.2019.02.046
32. Shamsollahi, H. R., Ghoochani, M., Jaafari, J., Moosavi, A., Sillanpää, M., & Alimohammadi, M. (2019b, June 15). Environmental exposure to endotoxin and its health outcomes: A systematic review. Ecotoxicology and Environmental Safety. Academic Press. https://doi.org/10.1016/j.ecoenv.2019.02.046
33. Thorne, P. S. (2021, July 1). Environmental endotoxin exposure and asthma. Journal of Allergy and Clinical Immunology. Mosby Inc. https://doi.org/10.1016/j.jaci.2021.05.004
34. Yadav, K., Yadav, A., & Kumar, R. (2026). A bibliometric analysis of research trends and patterns on ambient airborne endotoxin exposure in communities. Next Research, 5, 101305. https://doi.org/10.1016/j.nexres.2026.101305
35. Yoda, Y., Tamura, K., & Shima, M. (2017). Airborne endotoxin concentrations in indoor and outdoor particulate matter and their predictors in an urban city. Indoor Air, 27(5), 955–964. https://doi.org/10.1111/ina.12370

Figures

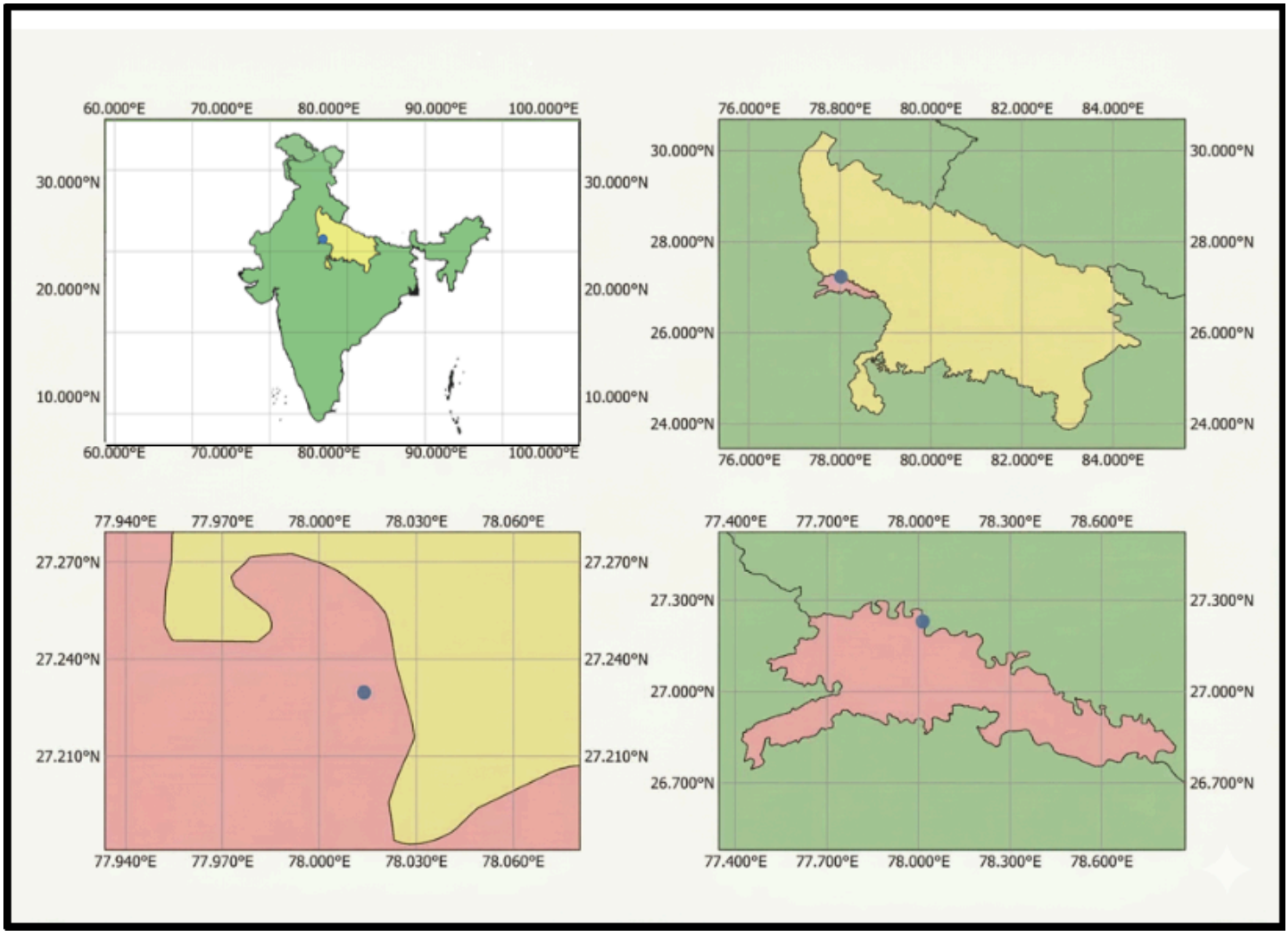

Figure 1

Study Site

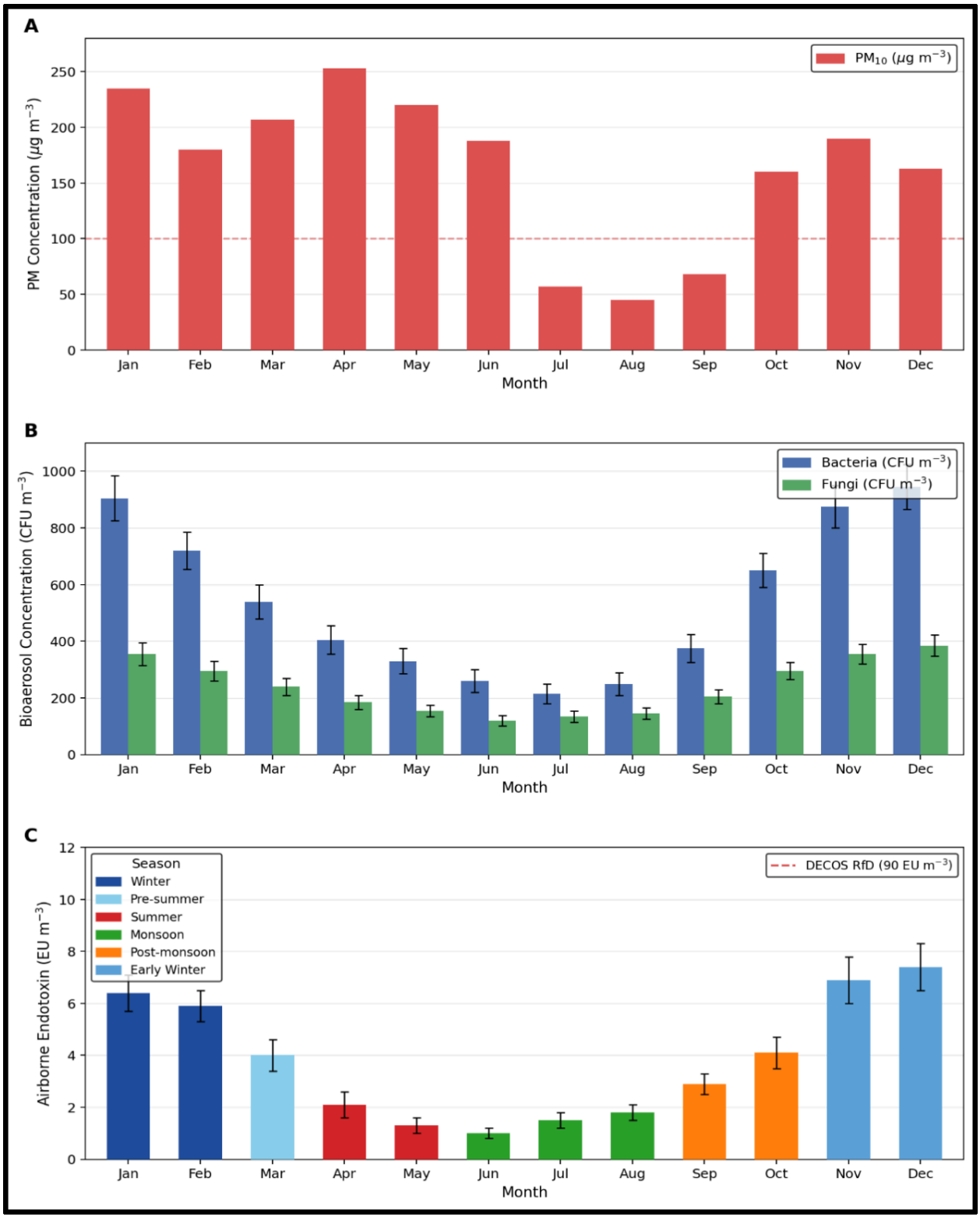

Figure 2

Monthly variation in particulate matter, bioaerosols, and airborne endotoxin concentrations during the study period. (A) Monthly mean concentrations of PM_{10} and $PM_{2.5}$ (μg m^{-3}); dotted lines indicate the National Ambient Air Quality Standards (NAAQS) limits for PM_{10} (100 μg m^{-3}). (B) Monthly mean concentrations of airborne bacteria and fungi (CFU m^{-3}) with standard deviation error bars. (C) Seasonal and monthly variation

of airborne endotoxin concentrations (EU m^{-3}) with associated standard deviations; the dashed red line represents the DECOS recommended reference limit of 90 EU m^{-3}.

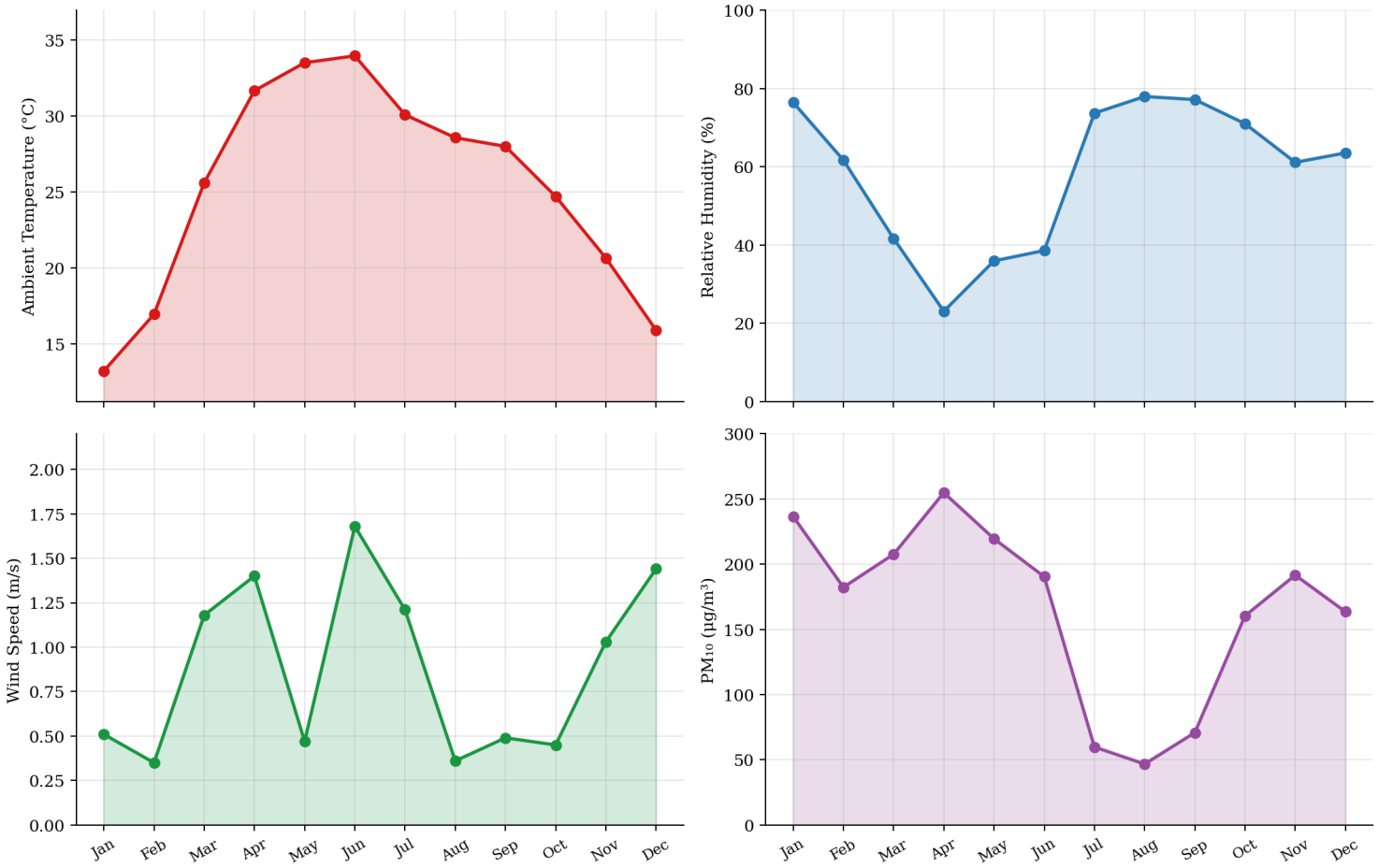

Figure 3

Seasonal profiles of meteorological parameters (temperature, RH, wind speed) and their co-variation with PM_{10}.

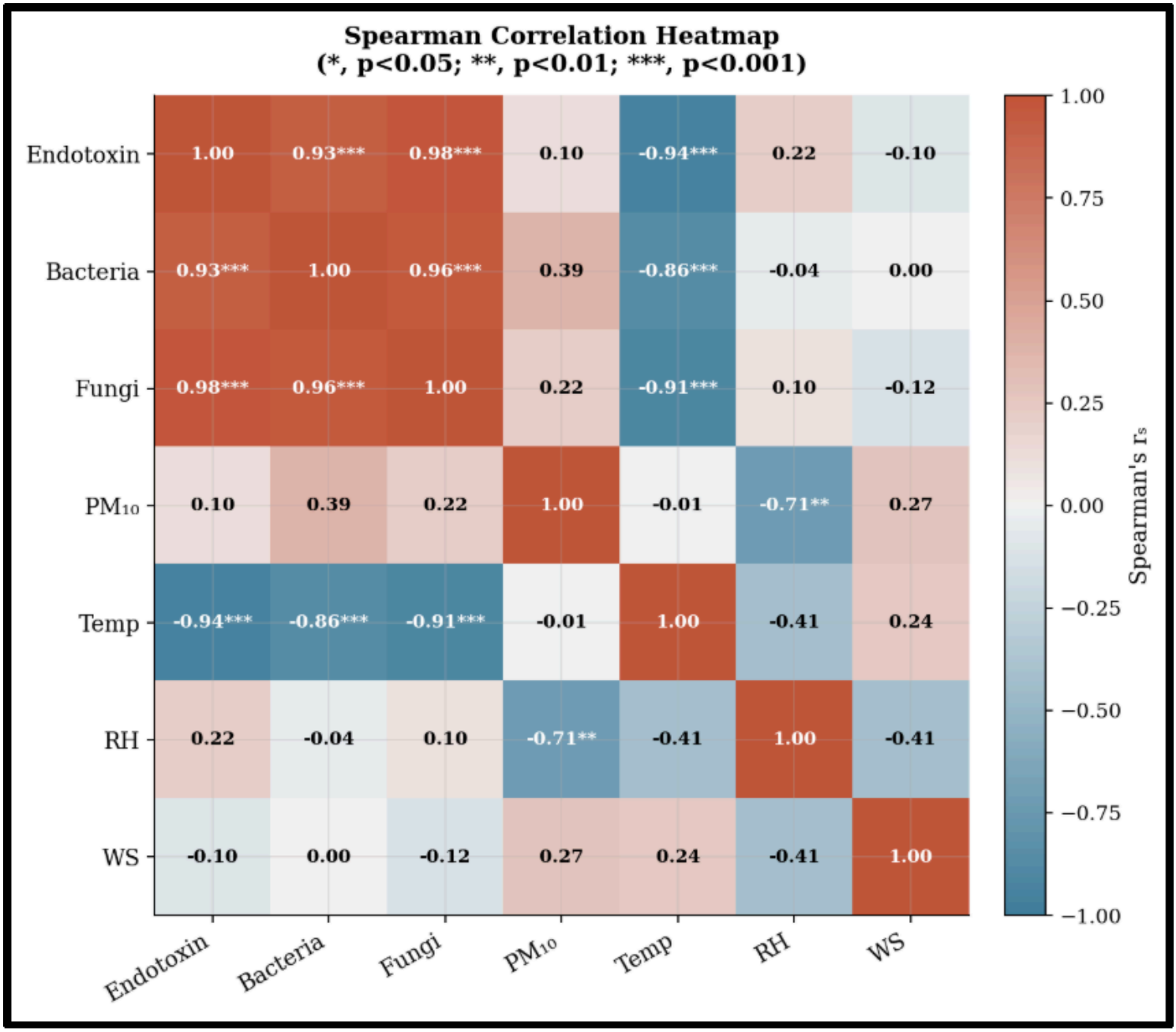

Figure 4

Spearman correlation heatmap illustrating relationships among endotoxin, bioaerosols, PM, and meteorological parameters.

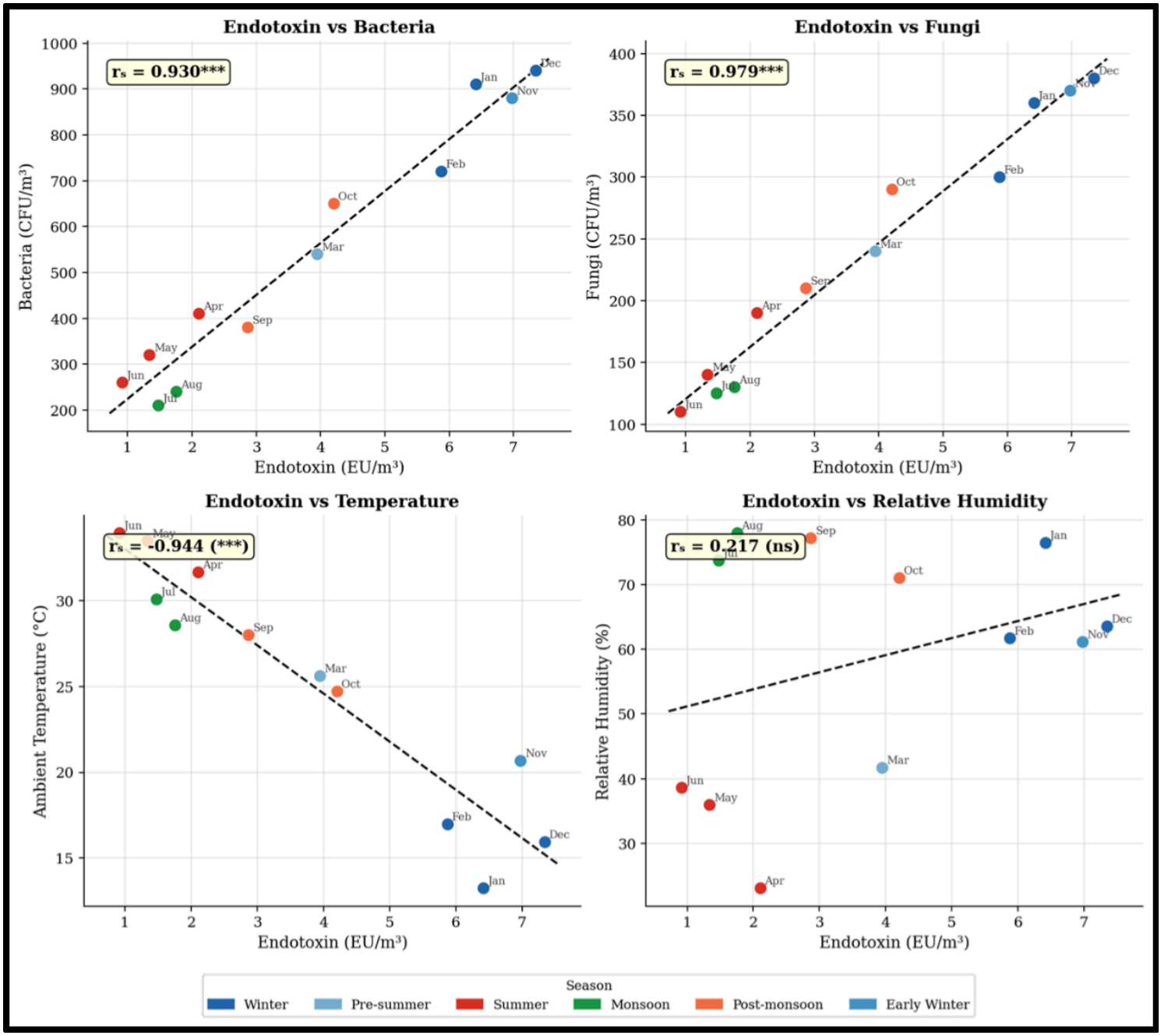

Figure 5

Scatter relationships between endotoxin and bioaerosols (bacteria and fungi) with regression trends.

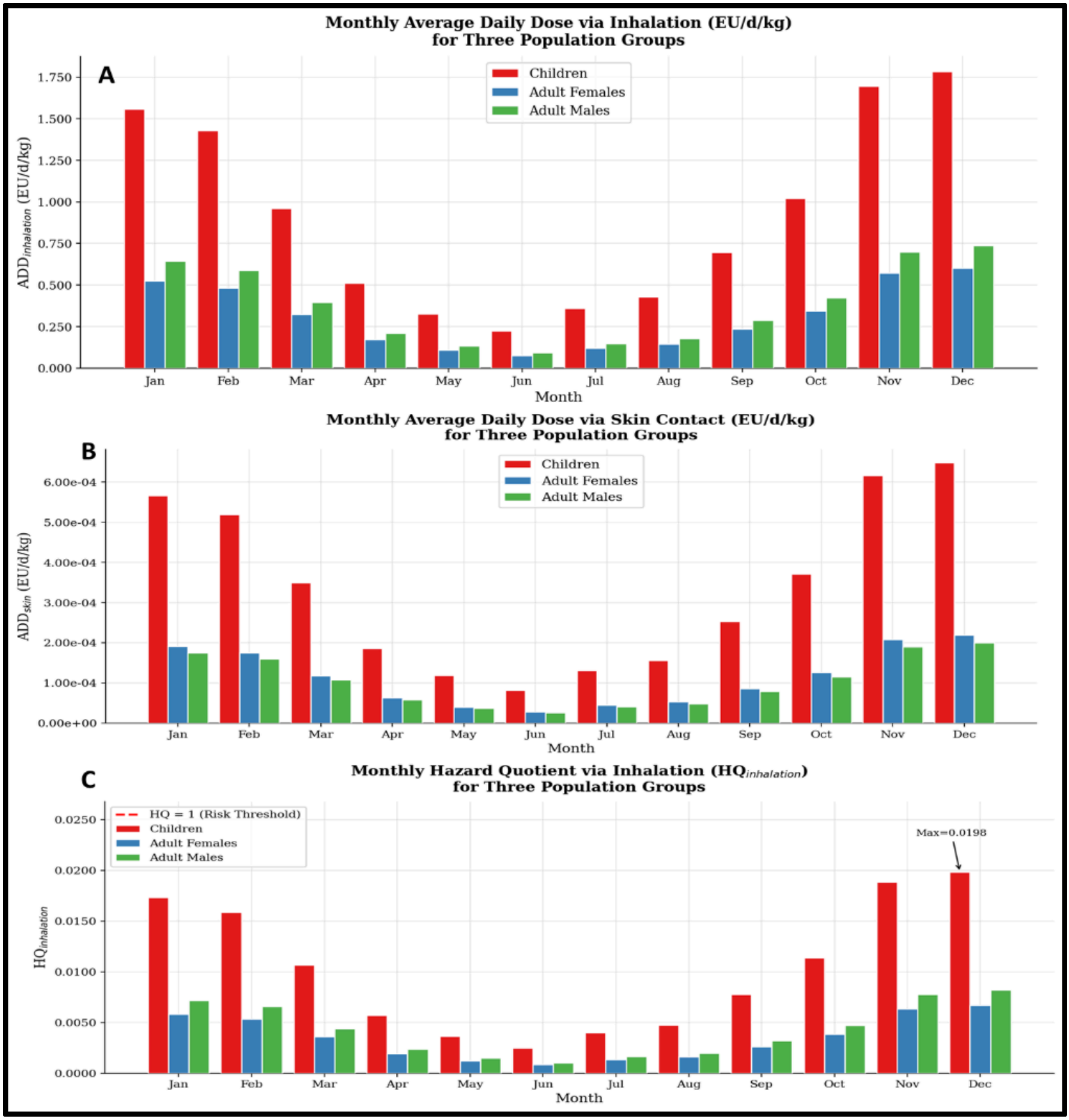

Figure 6

Monthly variation in exposure dose and health risk assessment of airborne endotoxins for different population groups. (A) Average daily dose via inhalation ($ADD_{inhalation}$, EU/d/kg), (B) average daily dose via skin contact (ADD_{skin}, EU/d/kg), and (C) hazard quotient via inhalation ($HQ_{inhalation}$) for children, adult females, and adult males. Children exhibited the highest exposure and risk levels across all months, with peak values

observed during winter and post-monsoon periods, while minimum values occurred during the monsoon season.

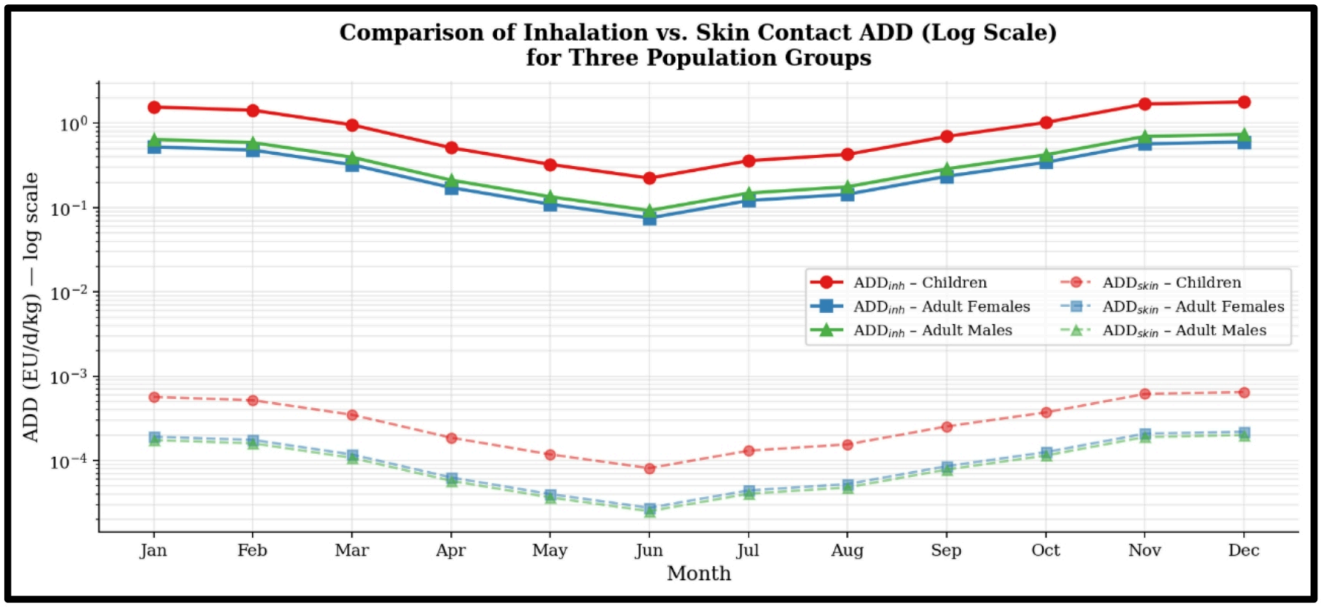

Figure 7

Log-scale comparison of inhalation vs dermal exposure pathways demonstrating pathway dominance.